David Taylor Research Center
Bethesda, MD 20084–5000

DTRC–PAS–90/15 April 1990

Propulsion and Auxiliary Systems Department
Research & Development Report

Flow Coupling Between a Rotor and a Stator in Turbomachinery

by
Yu-Tai Lee
Ivan Chen Wen Jiang
Thomas W. Bein

DTRC–PAS–90/15 Flow Coupling Between a Rotor and a Stator in Turbomachinery

MAJOR DTRC TECHNICAL COMPONENTS

CODE 011 DIRECTOR OF TECHNOLOGY, PLANS AND ASSESSMENT

12 SHIP SYSTEMS INTEGRATION DEPARTMENT

14 SHIP ELECTROMAGNETIC SIGNATURES DEPARTMENT

15 SHIP HYDROMECHANICS DEPARTMENT

16 AVIATION DEPARTMENT

17 SHIP STRUCTURES AND PROTECTION DEPARTMENT

18 COMPUTATION, MATHEMATICS & LOGISTICS DEPARTMENT

19 SHIP ACOUSTICS DEPARTMENT

27 PROPULSION AND AUXILIARY SYSTEMS DEPARTMENT

28 SHIP MATERIALS ENGINEERING DEPARTMENT

DTRC ISSUES THREE TYPES OF REPORTS:

1. **DTRC reports, a formal series,** contain information of permanent technical value. They carry a consecutive numerical identification regardless of their classification or the originating department.

2. **Departmental reports, a semiformal series,** contain information of a preliminary, temporary, or proprietary nature or of limited interest or significance. They carry a departmental alphanumerical identification.

3. **Technical memoranda, an informal series,** contain technical documentation of limited use and interest. They are primarily working papers intended for internal use. They carry an identifying number which indicates their type and the numerical code of the originating department. Any distribution outside DTRC must be approved by the head of the originating department on a case-by-case basis.

NDW-DTNSRDC 5602/51 (Rev 2-88)

REPORT DOCUMENTATION PAGE

1a. REPORT SECURITY CLASSIFICATION Unclassified	1b. RESTRICTIVE MARKINGS
2a. SECURITY CLASSIFICATION AUTHORITY	3. DISTRIBUTION/AVAILABILITY OF REPORT Approved for public release; distribution is unlimited.
2b. DECLASSIFICATION/DOWNGRADING SCHEDULE	
4. PERFORMING ORGANIZATION REPORT NUMBER(S) DTRC-PAS-90/15	5. MONITORING ORGANIZATION REPORT NUMBER(S)
6a. NAME OF PERFORMING ORGANIZATION David Taylor Research Center 6b. OFFICE SYMBOL (If applicable) Code 2722	7a. NAME OF MONITORING ORGANIZATION
6c. ADDRESS (City, State, and ZIP Code) Annapolis, MD 21402	7b. ADDRESS (City, State, and ZIP Code)
8a. NAME OF FUNDING/SPONSORING ORGANIZATION Office of Naval Technology 8b. OFFICE SYMBOL (If applicable) ONT 211 & 233	9. PROCUREMENT INSTRUMENT IDENTIFICATION NUMBER
8c. ADDRESS (City, State, and ZIP Code) Arlington, VA 22217-5000	10. SOURCE OF FUNDING NUMBERS PROGRAM ELEMENT NO.: 62121N, 62323N PROJECT NO.: RH21E44, RB23P11 TASK NO.: WORK UNIT ACCESSION NO.: 1-2720-102, 1-2720-104

11. TITLE (Include Security Classification)

Flow Coupling Between a Rotor and Stator in Turbomachines

12. PERSONAL AUTHOR(S)

Yu-Tai Lee, Ivan Chen Wen Jiang, and Thomas W. Bein

13a. TYPE OF REPORT	13b. TIME COVERED	14. DATE OF REPORT (YEAR, MONTH, DAY)	15. PAGE COUNT
Phase	FROM _____ TO _____	April 1990	24

16. SUPPLEMENTARY NOTATION

This paper has been submitted to The Third International Symposium on Transport Phenomena and Dynamics of Rotating Machinery (ISROMAC-3) Honolulu, Hawaii, USA, April 1-4, 1990).

17. COSATI CODES		
FIELD	GROUP	SUB-GROUP

18. SUBJECT TERMS (Continue on reverse if necessary and identify by block number)

Potential flow, Lifting surface, Stator, Rotor, Interaction, Performance, Turbomachine

19. ABSTRACT (Continue on reverse if necessary and identify by block number)

The structure of the flow in a turbomachinery passage is extemely complex. Successful turbomachine design requires detailed information about the flow characteristics in order to predict the performance of a candidate geometry. The designer needs information about the complex interaction between the blade rows when multistage blade rows are considered. A three-dimensional steady potential-flow code for a single blade row has been developed, where integral equations were derived to model the solid surfaces and the inlet condition for both external and internal flows with rotating or nonrotating lifting blades. Global iterations for the surface-panel source densities and the vortex strengths were used in conjunction with a Neumann iteration for solving the integral equations. In this paper, two numerical coupling procedures between the rotor and the stator are described. The phenomena of flow interaction between the rotor and the stator are studied and two test cases are presented. The performance of a vaneaxial fan is predicted using this procedure and the results indicate that the present numerical coupling procedure can be used by designers to select optimal blade shapes.

20. DISTRIBUTION/AVAILABILITY OF ABSTRACT	21. ABSTRACT SECURITY CLASSIFICATION
☒ UNCLASSIFIED/UNLIMITED ☐ SAME AS RPT ☐ DTIC USERS	Unclassified

22a. NAME OF RESPONSIBLE INDIVIDUAL	22b. TELEPHONE (Include Area Code)	22c. OFFICE SYMBOL
Thomas W. Bein	(301) 267-3644	Code 2722

DD FORM 1473, JUN 86 *Previous editions are obsolete.*

TABLE OF CONTENTS

FIGURES

ABBREVIATIONS

$d\ell$ - Line segment, ft

dS - Differential surface element, ft^2

f - Scalar function

ft - Feet

g - Gravitational constant, 32.17 (ft lbm)/(lbf sec^2)

gpm - Gallons per minute

H - Fluid head, ft

K - Kernel of the integral equation

lbf - Pounds force

lbm - Pounds mass

L - Line integral

M - Strength of surface source singularity, ft^3/sec

M(P) - Strength of surface source at P, ft^3/sec

M(Q) - Strength of surface source at Q, ft^3/sec

N - Surface normal, ft

Q - Flowrate, gpm

$\mathbf{r}_{PQ}$ - Position vector between points P and Q, ft

r_{PQ} - Distance between points P and Q, ft

r_i, r_o - Radius of inlet and outlet, ft

$\mathbf{V}$ - Velocity, ft/sec

$\mathbf{V}_M$ - Velocity due to source M, ft/sec

$\mathbf{V}_{EM}$ - Velocity due to external singularity M, ft/sec

$\mathbf{V}_\Gamma$ - Velocity due to the vortex Γ, ft/sec

V_r, V_θ, V_z - Radial, tangential and axial components of velocity, ft/sec

S - Boundary surface, ft^2

S_i, S_o - Inlet and outlet surfaces, ft^2

T_F - Fluid torque, (ft lbf)

x, y, z - Cartesian coordinates, ft

α_o - Solid angle, radians

Γ - Strength of vortices, ft^2/sec

Γ_o - Prerotation strength, ft^2/sec

π - Trigonometric constant, 3.14159...

ρ - Fluid density, lbm/ft^3

ϕ - Scalar potential, ft^2/sec

ω - Angular speed, revolutions per minute

SUBSCRIPTS

A - Axial direction

M - Source singularity

N - Surface normal

P,Q - Field points

t - Trailing edge

T - Tangential direction

∞ - Free stream

ABSTRACT

The structure of the flow in a turbomachinery passage is extremely complex. Successful turbomachine design requires detailed information about the flow characteristics in order to predict the performance of a candidate geometry. The designer needs information about the complex interaction between the blade rows when multistage blade rows are considered. A three-dimensional steady potential-flow code for a single blade row has been developed, where integral equations were derived to model the solid surfaces and the inlet condition for both external and internal flows with rotating or nonrotating lifting blades. Global iterations for the surface-panel source densities and the vortex strengths were used in conjunction with a Neumann iteration for solving the integral equations. In this paper, two numerical coupling procedures between the rotor and the stator are described. The phenomena of flow interaction between the rotor and the stator are studied and two test cases are presented. The performance of a vaneaxial fan is predicted using this procedure and the results indicate that the present numerical coupling procedure can be used by designers to select optimal blade shapes.

ADMINISTRATIVE INFORMATION

This research was sponsored jointly by the Independent Research and Independent Exploratory Development Program, DN 509501 Element 62936N, and by the Office of Naval Technology Submarine and Surface Ship Auxiliary Systems Exploratory Development Projects, Program Elements PE62323N Block ND3A and PE62121N Block ND1A, administered by the David Taylor Research Center.

INTRODUCTION

The design of turbomachines has for many years been supported by an ever increasing volume of information on the performance aspects of the machines. This information is concerned primarily with the fluid flow problems of cascades and the meridional flow through the multiplicity of blade rows in axial-flow compressors and turbines.

There are basically two recognized forms of interaction between rotor and stator blade rows. One is due to the wakes behind blades or other elements of the machine immersed in the flow due to viscous effects, and the other is due to potential-flow effects which would occur if the working fluid were perfectly inviscid. All observations made in practical situations represent a combination of the two sources which it has not been possible to separate except on the basis of some assumed knowledge of the mechanisms involved. Reference [1] provides an example of an axial flow turbomachine that uses both upstream inlet-guide-vanes and a downstream stator with the rotor. The blades on the rotor operated at high relative velocity and could therefore be expected to have intense wakes. Removal of the downstream stator on which the rotor wakes could have reacted produced a slightly measurable reduction in the noise level. Removal of the inlet-guide-vane, however, produced remarkable noise reductions. This example indicates the significance of the potential-flow interaction effect between the inlet-guide-vane and the rotor.

Recently, Navier-Stokes solution procedures have been used by researchers [2,3] in seeking viscous solutions for interacting flows for a rotor-stator operating in the compressible range. Detailed flow and heat-transfer information can be obtained. Efforts for obtaining these solutions are tremendous. Extension of these approaches to incompressible flows or more complex geometries, e.g. asymmetric blade row, is not a straight forward task and solution strategies have not been practical.

This paper uses a previously developed three-dimensional steady potential-flow code [4] for a single rotating or nonrotating blade row to examine the potential-flow effects between rotor and stator. A numerical coupling of the rotor-stator influence is developed. A mathematically defined centrifugal machine and an actual axial-flow fan were used to demonstrate the present scheme for predicting machine performance.

THEORY

Single-Blade-Row Calculation

A potential-flow solution model is developed to investigate the rotor-stator interaction. This potential-flow model utilizes a surface-singularity method for the representation of a nonpenetrating surface condition, and an inviscid vortex-line distribution for the representation of a lift-generation blade [4]. The surface singularities used are constant-strength sources or sinks on each panel. Thus the computed flow field in terms of the strengths of the surface singularities (M) and the vortices (Γ) is

where ϕ is a scalar potential for the resultant potential-flow field, M(Q) and Γ(Q) are the strengths of the source and the vortex, and r_{PQ} is the distance between a field point P and a source/vortex point Q. A Fredholm integral equation of the second kind for the unknown M(Q) is formulated as

$$2\pi\, M(P) = f(P) + \int_S [\, M(Q)\, K(P,Q) - M(P)\, K(Q,P)\,]\, dS_Q + [\, 2\pi - \alpha_o(P)\,]\, M(P), \tag{4}$$

and

$$K(P,Q) = \frac{\partial}{\partial N_P}\,\frac{1}{r_{PQ}},$$

$$\alpha_o(P) = \int_{S_o} K(Q,P)\, dS_Q,$$

$$f(P) = V_N(P) - V_{TN}(P),$$

where K(Q,P) is the transpose of the kernel of K(P,Q), N is the surface normal directed into the flow field, V_N is the N-component velocity due to blade rotation and incoming flow, and V_{TN} is the N-component velocity due to vortices. The vortex strength is determined by using the Kutta condition near the trailing edge of the blade. In this paper a wake tangency condition is satisfied at the Kutta point. The vortex wake structure generally adopts a helix shape. Its modelling for moving and nonmoving blades is given in Appendix A. A global iteration scheme [4] is developed for solving both the unknown strengths of sources and vortices.

Rotor-Stator Coupling

Flow past an axial-flow or a centrifugal single-stage rotor and stator is truly unsteady and asymmetric. The circumferential mean of the flow field between the blades of each blade row, however, can be represented by a steady, symmetric nonuniform through flow. This mean flow can then be used in the performance calculation. The single-blade-row calculation, described in the previous section, is suitable for predicting the flow field with this symmetric nonuniform inlet condition.

The coupling between the rotor and the stator can be modelled by considering either the stator or the rotor as a group of external singularities which exert an influence on the other one. Therefore when the flow in the rotor (or stator) is calculated, it experiences an effect from the singularities outside the rotor (or stator). To include this effect, the first term on the right hand side of Eq. (4) is modified as:

$$f(P) = V_N(P) - V_{TN}(P) - V_{EXN}(P), \qquad (5)$$

where V_{EN} is the N-component velocity due to external singularities. The complete calculation is accomplished by an iterative scheme. Initially the symmetric flow in the rotor is calculated using the single-blade-row model, then the asymmetric stator flow, due to relative position of rotor and stator passages, is calculated considering the calculated rotor singularities as a set of external singularities. After completing the stator flow field calculation, the first iteration is completed. The second iteration of the rotor starts with the influence from the external singularities of the stator and the influence from the now asymmetric flow between the rotor and the stator. A similar calculation is made for the stator flow field to complete the second iteration. This iterative procedure can be carried on until a converged solution is obtained. The sources and vortex of each blade are adjusted during the calculations to account for the effect of the asymmetric flow. This procedure generally requires large computer memory and computing time for each rotor or stator calculation. A single stage centrifugal pump geometry with mathematically defined blades is used in this paper to demonstrate this approach.

In an effort to reduce the computing time and memory required for the previous approach, a technique was developed that takes advantage of the periodic mean flow field through the rotor and the stator. After the initial symmetric rotor solution is obtained, conservation of rotational energy is preserved between the rotor exit flow and the stator inlet flow. A preswirl strength, derived in Appendix B, is calculated. This preswirl strength is added to a symmetric stator flow field to preserve the energy imparted by the rotor. Although the calculated rotor exit flow is nonuniform in the tangential direction between rotor blades, an averaging of the calculated velocities is performed in the tangential direction at each radius. Therefore, the stator inlet flow becomes a nonuniform axial flow in the radial direction combined with a preswirl strength. These inlet conditions enable the

stator flow field calculation to be considered as axisymmetric. For the second iteration, the external singularity effect from the calculated stator solutions is added to the rotor flow field calculations. The induced velocity on each rotor control point is calculated from the singularities of the stator. Then the boundary conditions for the rotor solutions are updated by Eq.(5). Since the velocity contribution from the external singularities in Eq.(5) decays with $1/r^2$, a symmetric influence from the stator singularities to the rotor blade row is assumed. Results for an actual one-stage axial-flow fan using this simplified procedure are given in the following section.

RESULTS

Mathematical Blade Rows

In Fig. 1, the geometry of the impeller and the diffuser for a single stage centrifugal pump is defined. The five-blade impeller rotates at ω rpm, but the seven-blade diffuser is stationary. Simple blade shapes with zero camber for both the impeller and the diffuser are selected for ease of geometry generation and numerical calculation. The hub and shroud are horizontal and parallel to the xy-plane. There is no inlet pipe. However, the inlet swirling effect in the impeller entrance is included by the prerotation Γ_o. The mesh pattern shown in Fig. 2 is for one complete repeating sector, which covers 60 degrees for the impeller, and 51.43 degrees for the diffuser, on the hub. There are 938 and 688 panels for the impeller and diffuser meshes, respectively. Due to the resemblance to a 2-D blade, a single-bound-vortex model without trailing vortices is used here for simplicity. The bound vortices are located at x = 0.425 ft and y = 0.075 ft for the impeller and x = 0.7 ft and y = 0.225 ft for the diffuser in Fig. 1. The Kutta points are at the middle points of the semicircles which form the blade trailing edges. Since an asymmetric flow calculation is adopted, only one Kutta point is used for each impeller or diffuser blade. The calculated relative impeller velocity distributions, for the case $V_{EMN} = 0$ in Eq.(5), are shown in Fig. 3. It shows the distributions for low, near-design and high flow cases. The alignment of the velocity vectors on the suction side of the rotor blade indicates that flow separation will occur even at the "design condition". This is due to the zero-camber blade used and would not be expected in a design with properly designed blades. At low flow condition, pressure-side separation is also indicated.

Three iterations were performed for the impeller-diffuser interaction. The final computed absolute velocity distribution is shown in Fig. 4. The convergence of the

solution procedure is monitored by the flow continuity calculations at both the impeller and the diffuser. Figure 5 shows the fluid mass recovery for the diffuser at Q = 1000 gpm. Since the flow control, i.e. inlet boundary condition, is at the inlet of the impeller, the flow continuity calculation is always well satisfied for the impeller. The continuity calculations for the diffuser show a smooth increase for each iteration to Q = 1000 gpm. The diffuser average flows at three different radii for each iteration are about 76, 91, and 97 percent of the impeller prescribed inlet flow. The variations of the calculated bound vortices and flow field are similar to the variations of the diffuser continuity calculations .

The fluid torque is calculated as the difference between the fluid angular momentum at the outlet and the inlet,

$$T_F = \rho \int_{S_o} V_r r_o V_\theta \, dS - \rho \int_{S_i} V_r r_i V_\theta \, dS, \qquad (6)$$

where S_o and S_i are the surfaces at the outlet and the inlet, V_r and V_θ are the radial and tangential velocity components, and ρ is the fluid density. The head change associated with the fluid torque is defined as

$$H = T_F \, \omega \, / \, \rho \, g \, Q, \qquad (7)$$

where g is the gravitational constant. Figure 6 shows the characteristics calculated according to Eqs. (6) and (7). The circle and the triangle are for the symmetric flow through the impeller at Γ_o = 0 and -50 ft^2/sec. The cross and the square are results from the impeller-diffuser interaction calculation at the impeller speed ω = 600 rpm, Q = 1000 gpm and Γ_o = 0. The cross (x) represents only the contribution across the impeller. The square is for the combined contribution of both the impeller and the diffuser. The results show that the fluid torque through the impeller for the impeller-diffuser unit is the same as that for the

impeller by itself. Due to the energy transfer from the kinetic to the potential energy in the diffuser, the overall fluid torque for the unit is reduced.

Axial-Flow Fan

A ventilation supply fan, with a 17-blade rotor and a 11-blade stator using the computational grid shown in Fig. 7, is used as a test example for validating the present simplified coupling procedures. Due to the requirement of the conservation of the rotational energy between the rotor and the stator, the solution converges rapidly. The continuity calculation indicates two iterations are adequate when overall flow quantities are concerned. After the second iteration, the rotor and the stator velocity distributions at ω = 3550 rpm and Q = 16,000 cfm are shown in Figs. 8 and 9, where the plotting locations for the velocity distributions are close to the blade trailing edges. These calculations were performed with the trailing vortex model described in Appendix A. The calculated vortex strengths across the spans of the rotor or the stator blades are very uniform. Due to the cancelation between the upper and lower horseshoe vortices, the results indicate that the blade flow at midspan can be closely modeled by a two-dimensional simulation. The tip and hub vortices are not cancelled and have a dominant effect on the calculated results. Effects from the tip and root vortices are shown in Figs. 8 and 9. Figure 10 shows the calculated pressure distributions on the rotor and stator blades. Again the tip and root vortices are responsible for the local jump in the pressure distributions. For other parts of the blades, the pressure distributions are generally uniform. The overall efficiency, defined as the ratio of the rotor energy transfer rate to the input electric energy (IHP), is calculated from the performance prediction and compared to the measured overall efficiency. Figure 11 shows a comparison between the calculated efficiency and the measured performance, which has a measurement

uncertainty of ±1.2%. Dependency of the numerical solution with grid size was given in reference [4] for the present model. Although the local calculated blade surface pressure between fine and coarse grids can vary up to 10%, the overall efficiency from the numerical results is estimated less than 4%. The comparison shown in Fig. 11 indicates that the loss due to the fluid energy transfer is small.

CONCLUSIONS

A computational scheme for coupling the flow field predicted by a potential-flow solution method for a rotor-stator combination has been developed. Two different coupling procedures have been evaluated: asymmetric and symmetric. The convergence of the asymmetric coupling approach was demonstrated by an impeller-diffuser geometry with mathematically defined blades. The symmetric averaging coupling approach was verified using an actual axial-flow fan. The predicted overall machine performance agrees well with the measured performance of the axial-flow fan. In conclusion, it has been shown that the simplified averaging approach can be used when overall averaged quantities of the flow field are sought. This technique is an important step in the development of the capability to design and analyze turbomachinery designs without having to fabricate and test each iteration. The result of this will be to increase the success rate while at the same time reducing the time and the cost to develop advanced turbomachinery for the Fleet.

ACKNOWLEDGEMENT

Thanks are due to Mr. L. Mulvihill for his initial contribution to the present work.

APPENDIX A

Modified Wake Vortex Model

The helix-shape trailing vortex model used in [4] for an axial-flow machine is given by Eq.(15) of [4],

$$x = r_t \sin\theta, \qquad y = r_t \cos\theta, \qquad z = z_t + V_\infty \theta / \omega, \tag{A1}$$

where the subscript t refers to the trailing edge, and θ is the azimuthal angle measured from the trailing edge. Equation (A1) can also be written as

$$\theta = \Delta z \, \omega / V_\infty, \tag{A2}$$

where Δz is the axial distance measured from t. This equation indicates that the helix is independent of the blade shape or inlet flow angle. A modified wake vortex model, which is suitable for moving as well as nonmoving blades, is used in the present calculation, i.e.

$$r_t \, \theta / \Delta z = (r_t \, \omega + V_{\infty Tt}) / V_{\infty At}, \tag{A3}$$

where subscripts A and T represent axial and tangential directions. Physically, this model relates the trailing vortex to the blade trailing edge velocities. There are two options added to this modified relation. First, a fixed flow exit angle at t can be specified. A relaxation parameter can be input to control the vortex recovery distance back to the state of incoming flow.

APPENDIX B

Stator Preswirl Model

The prerotation effect can be simulated by a line vortex along the axial direction from z = 0 to z = ∞. If the strength of this vortex is assumed to be constant Γ_o, the tangential velocity at P due to Γ_o is

$$V_\theta = \frac{\Gamma_o}{4\pi\, r_p} \left[1 + \frac{z_p}{(r_p^2 + z_p^2)^{\frac{1}{2}}} \right], \qquad \text{(B1)}$$

where r_p is the radius of point P from the center axis. When the conservation of rotational energy is applied to the rotor exit plane and the stator inlet plane,

$$\int_{S_o} V_z\, r_p\, V_\theta\, dS_p = \int_{S_i} V_z\, r_p\, V_\theta\, dS_p. \qquad \text{(B2)}$$

Substituting Eq.(B1) into Eq.(B2), one obtains

$$\Gamma_o = 4\pi \frac{\int_{S_o} V_z\, r_p\, V_\theta\, dS_p}{\int_{S_i} V_z \left[1 + \frac{z_p}{(r_p^2 + z_p^2)^{\frac{1}{2}}} \right] dS_p}. \qquad \text{(B3)}$$

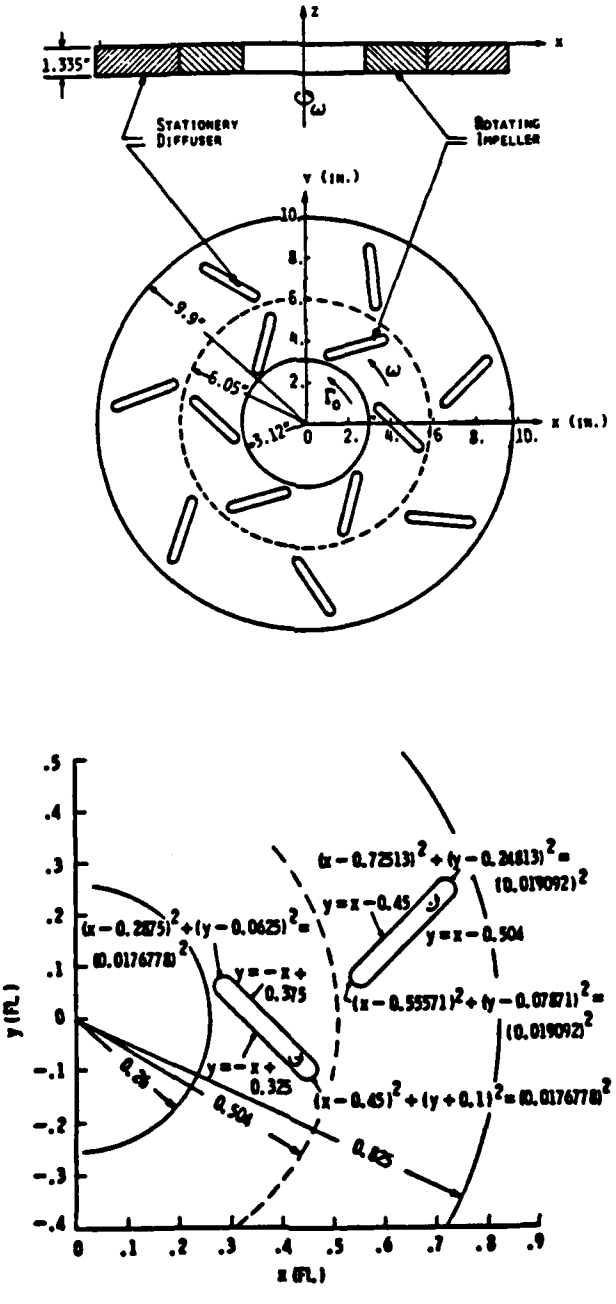

Figure 1. The Impeller-Diffuser Geometry

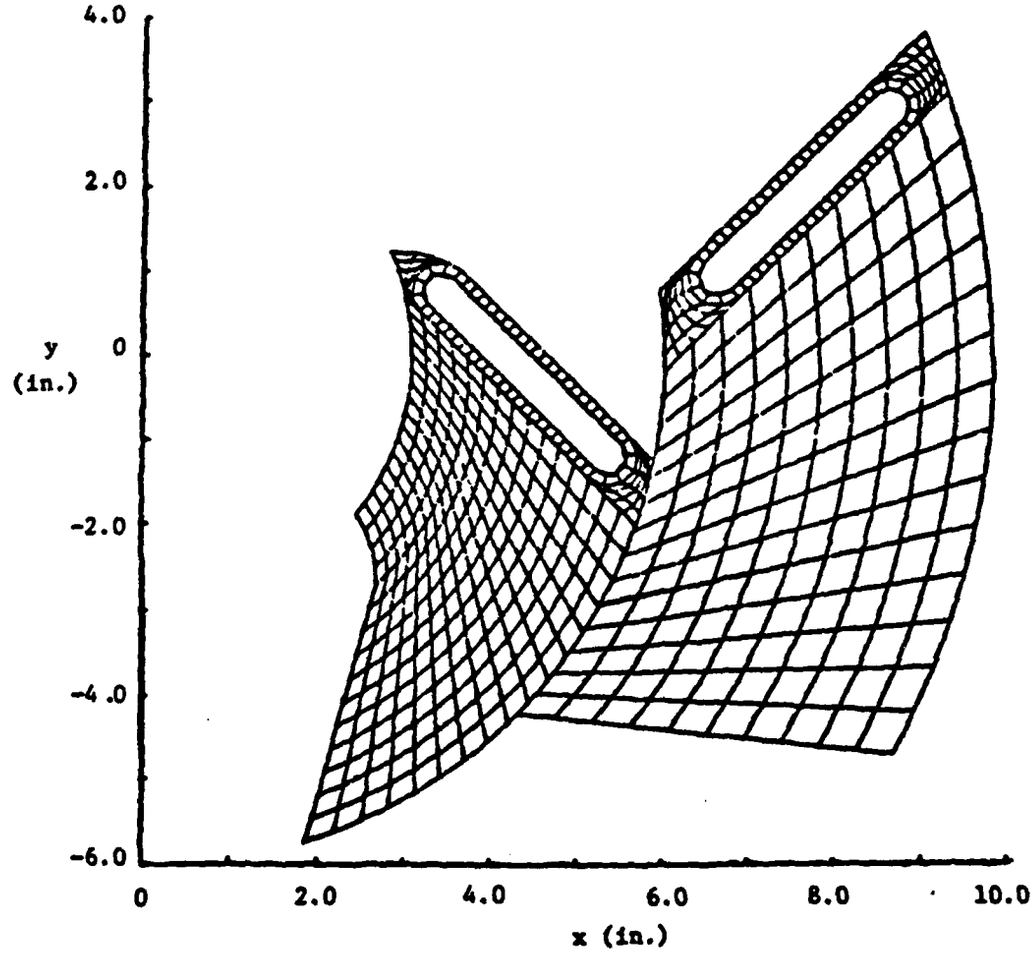

Figure 2. Surface Meshes on the Hub of the Impeller-Diffuser

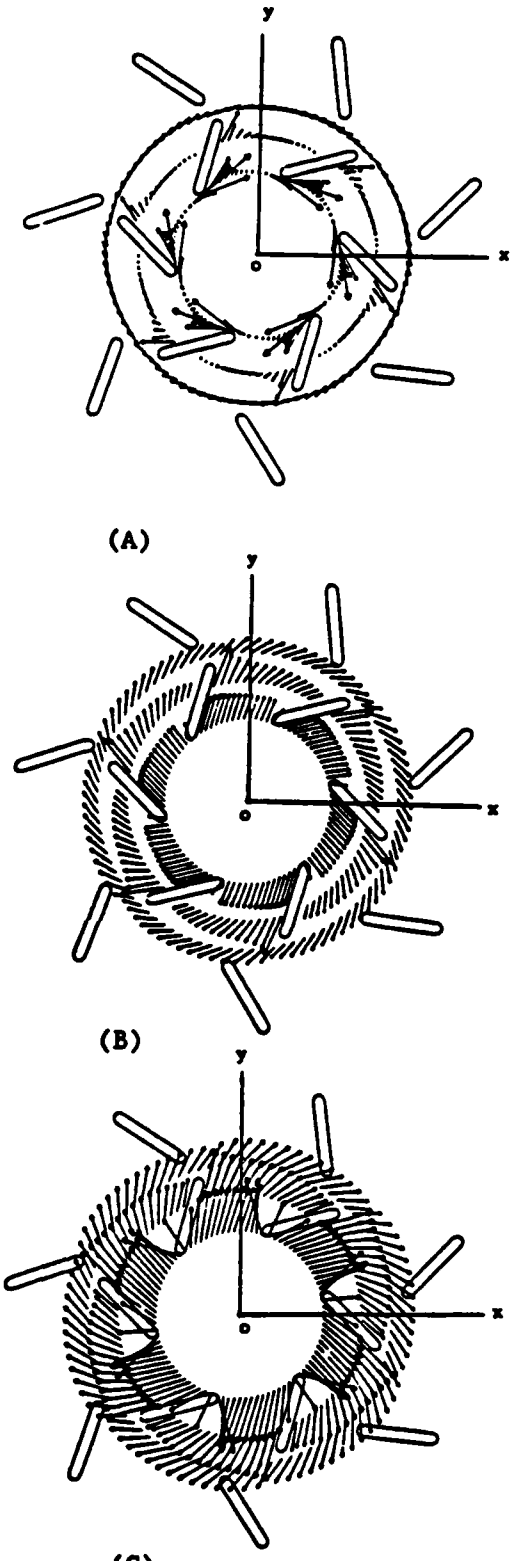

Figure 3. Relative Velocity Distributions at Midspan for the Symmetric Flow Past the Impeller, ω = 600 rpm, Γ_e = 0.
(A) Q = 400 gpm, (B) Q = 2500 gpm, (C) Q = 4400 gpm.

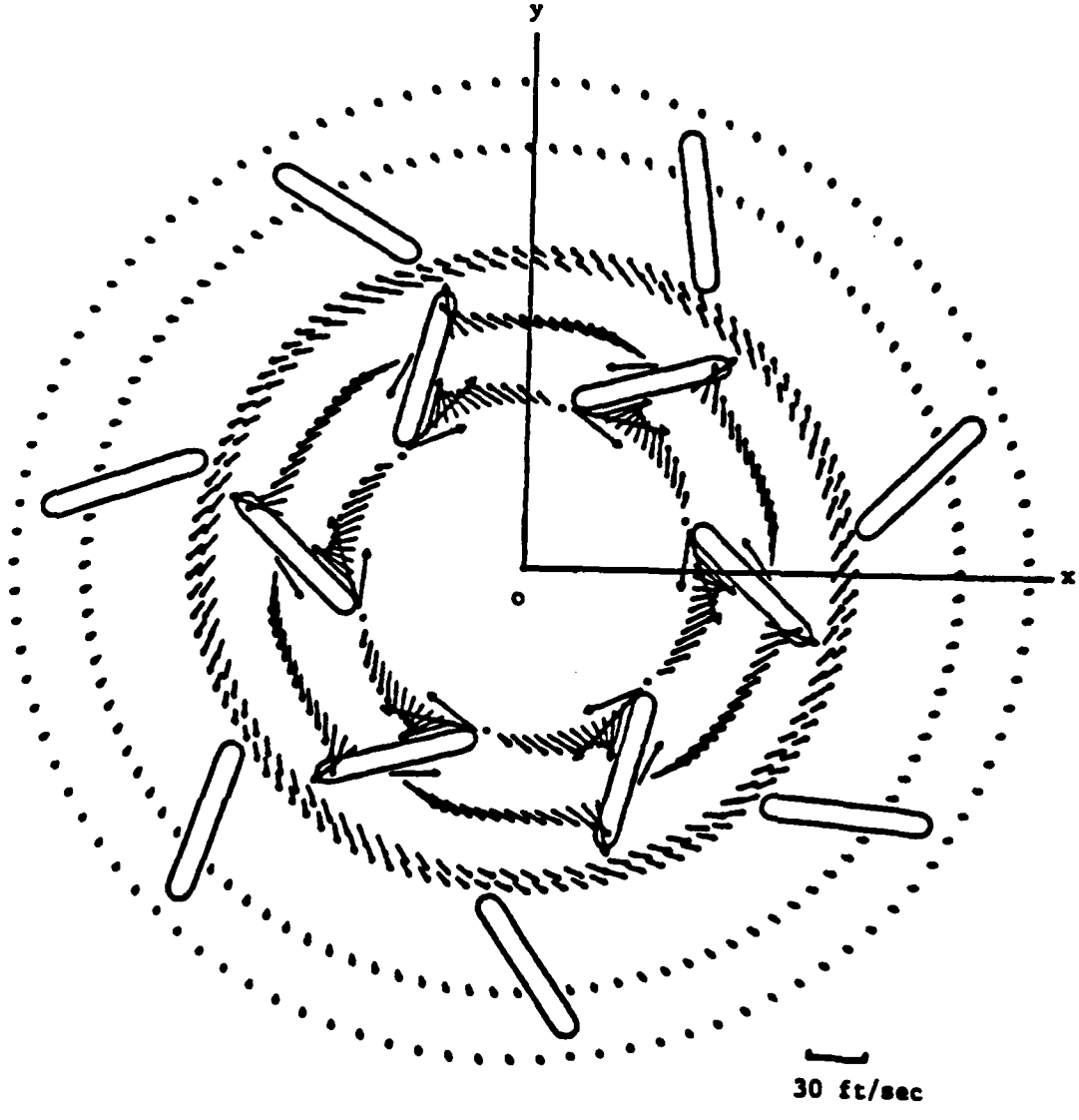

Figure 4. Absolute Velocity Distribution at Midspan for Flow Past the Impeller and the Diffuser After the Third Iteration, ω = 600 rpm, Q = 1000 gpm, Γ_o = 0.

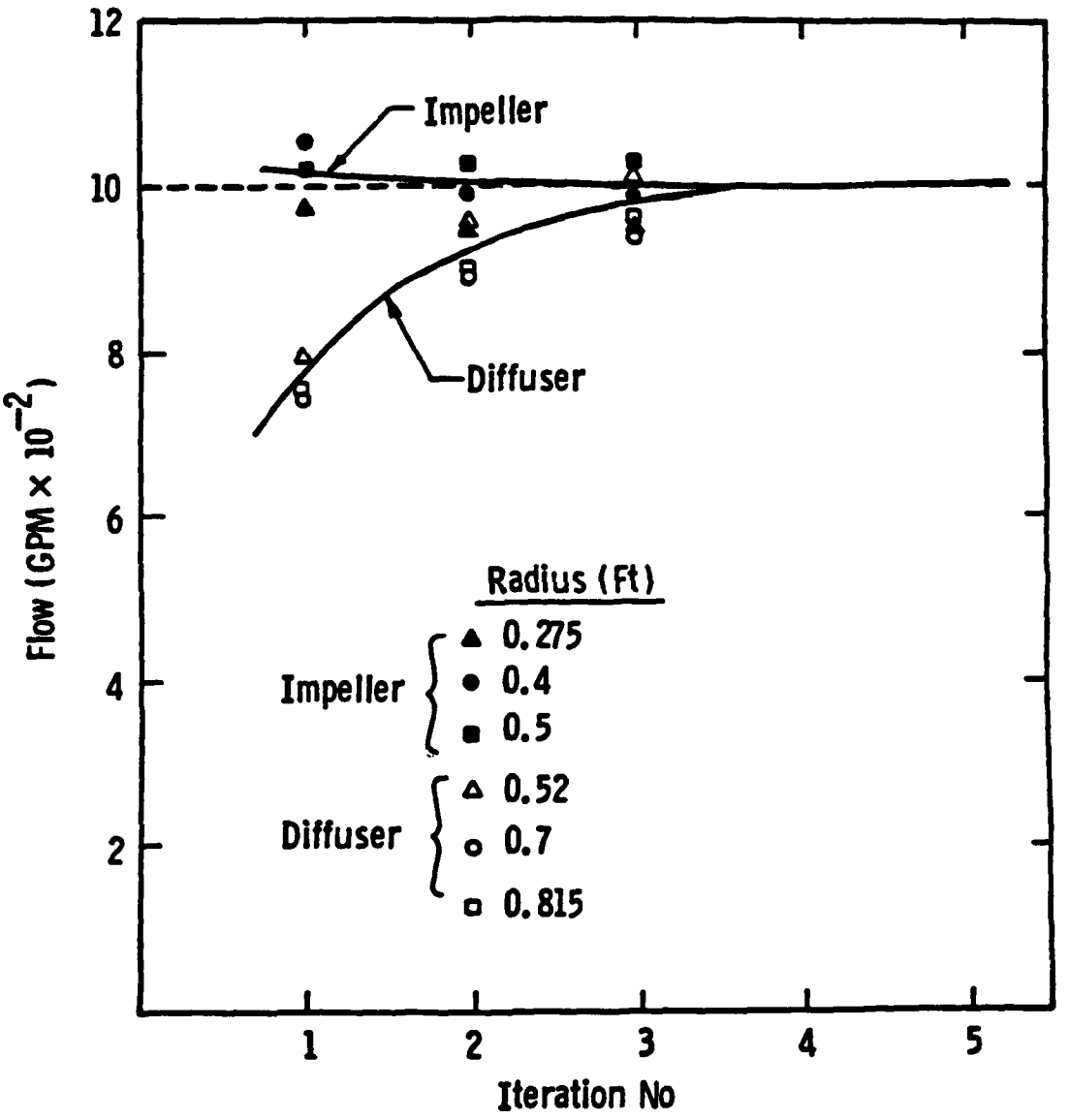

Figure 5. Flow Continuity Calculations at Different Radii Between Successive Iterations for Q = 1000 gpm.

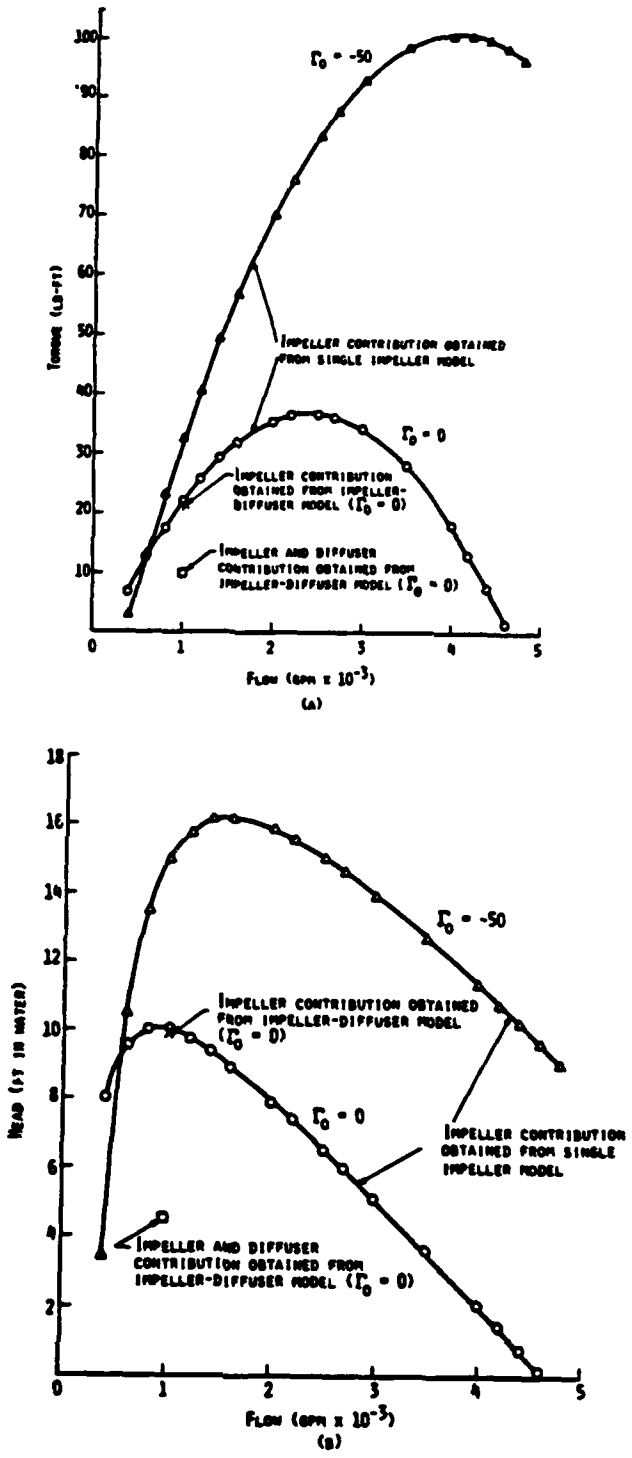

Figure 6. The Characteristics for the Impeller-Diffuser (A) Torque, (B) Head.

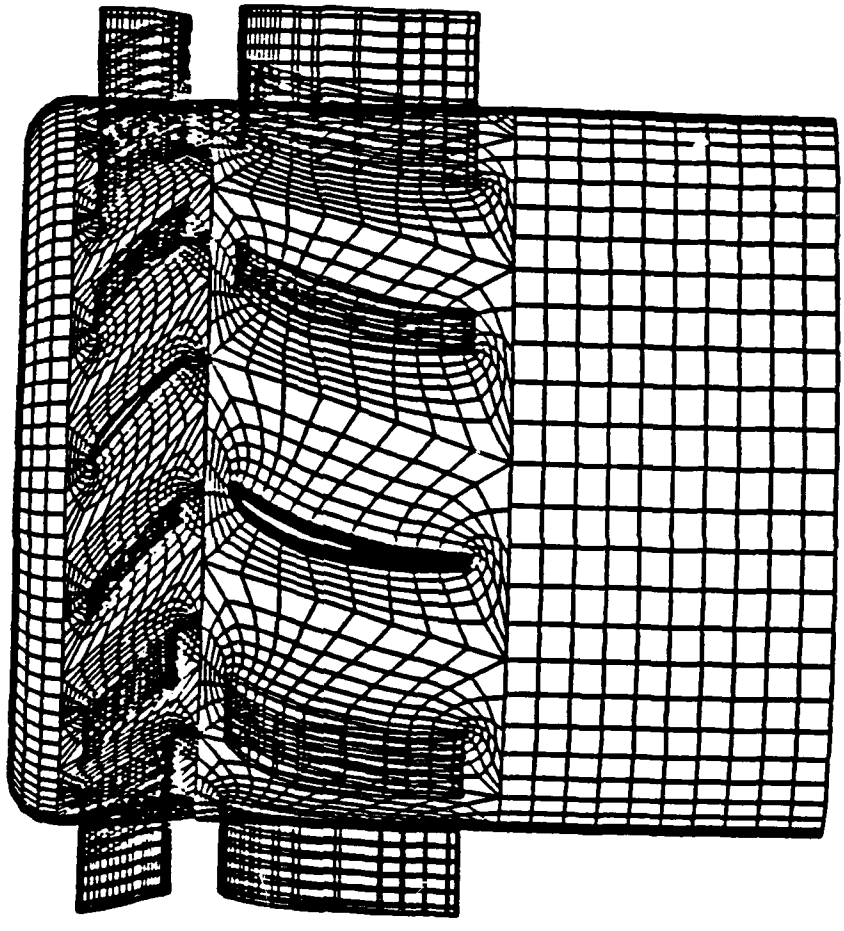

Figure 7. Computational Grid for the Air Supply Fan (Outside casing is not shown)

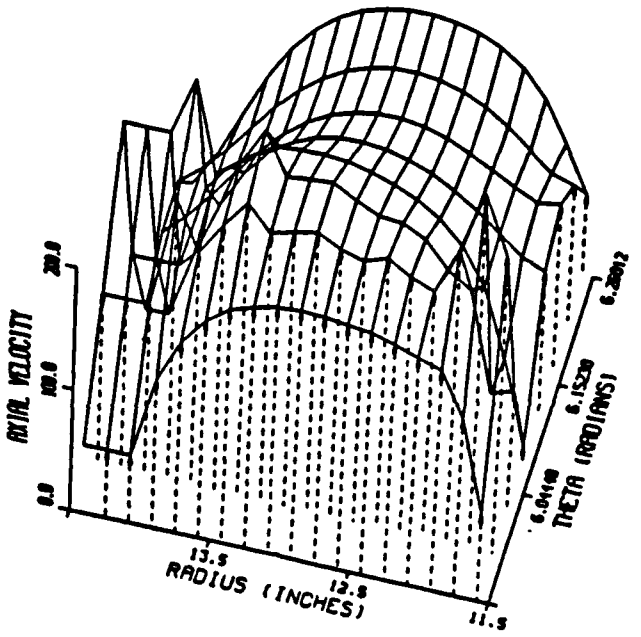

(A)

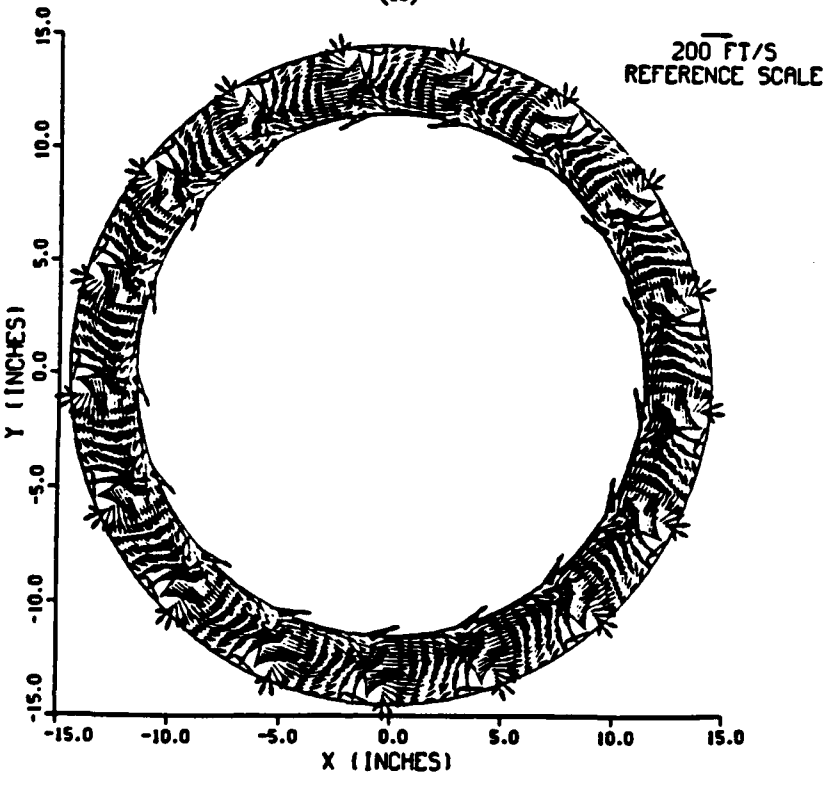

(B)

Figure 8. Rotor Velocity Distributions near Trailing Edge, ω = 3550 rpm, Q = 16,000 cfm, (A) Axial (B) Radial and Tangential Components.

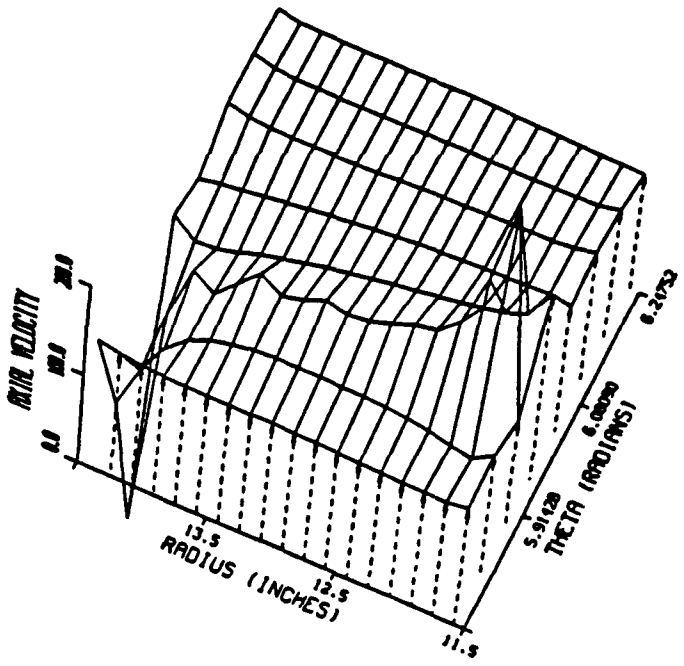

(A)

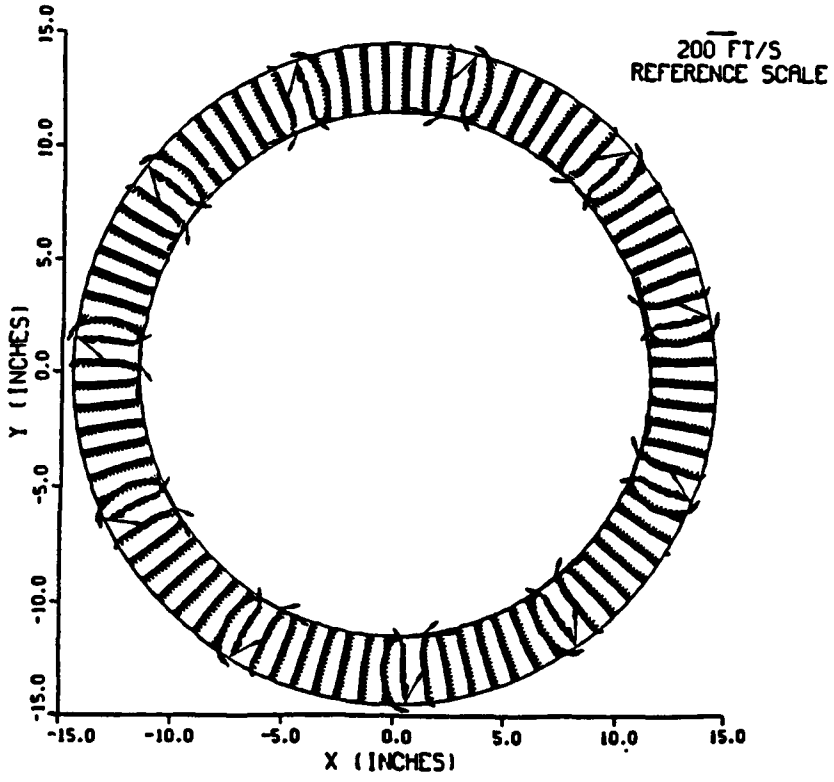

(B)

Figure 9. Stator Velocity Distributions near Trailing Edge, ω = 3550 rpm, Q = 16,000 cfm, (A) Axial (B) Radial and Tangential Components.

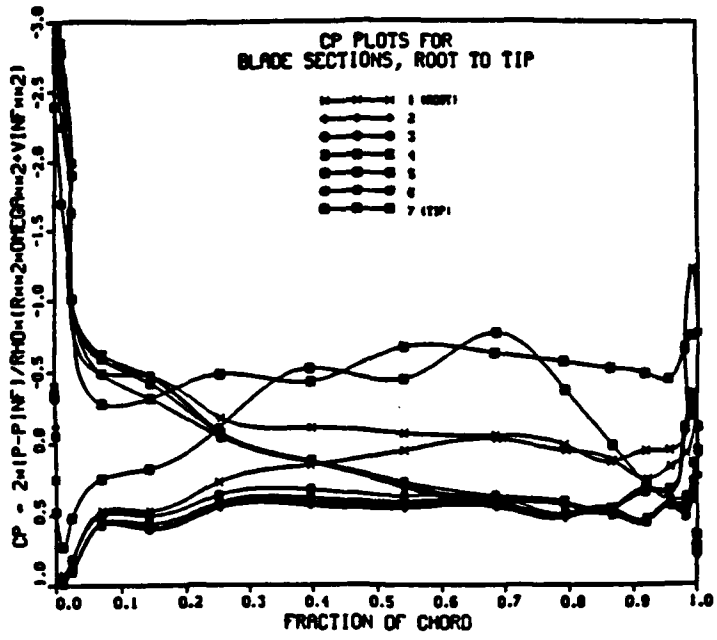

(A)

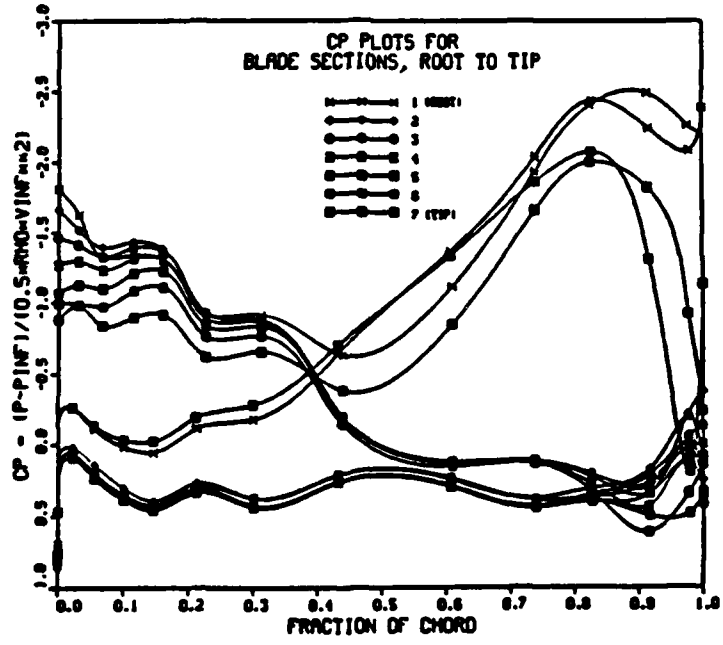

(B)

Figure 10. Calculated Blade Pressure Distributions for Single-Stage Ventilation Supply Fan, ω = 3550 rpm, Q = 16,000 cfm, (A) Rotor (B) Stator.

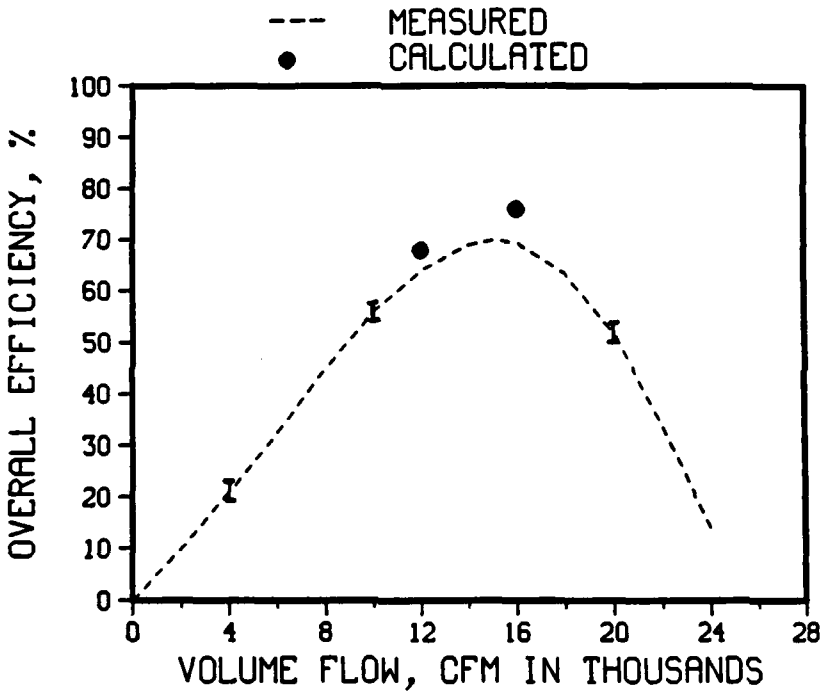

Figure 11. Performance Prediction for Single-Stage Ventilation Supply Fan

REFERENCES

[1] Rizk, W. and D.M. Seymour, "Investigation into the Failure of Gas Circulators and Circuit Components at Hinkley Point Nuclear Power Station," Proc. Inst. Mech. Engrs, Vol. 179, No.1, 1964-65.

[2] Rai, M.M., "Unsteady Three-Dimensional Navier-Stokes Simulations of Turbine Rotor-Stator Interaction," AIAA Paper 87-2058, 1987.

[3] Giles, M.B., "Stator/Rotor Interaction in a Transonic Turbine," AIAA Paper 88-3093, 1988.

[4] Lee, Y.T., C.W. Jiang and T.W. Bein, "A Potential Flow Solution on Marine Propeller and Axial Rotating Fan," DTRC Report 88/031, 1988.

INITIAL DISTRIBUTION

Copies

2 CNO

1 222

1 22T

6 ONT

1 21

1 21B

1 211 (Gagorik)

1 23 (Faulstitch)

1 23B (Fitch)

1 233 (Remmers)

1 ONR

1 113

8 NAVSEA

1 SEA 05R32 (Smookler)

1 SEA 08

1 SEA 5027

1 SEA 55W3 (Comstock)

1 SEA 55W31 (Jones)

1 SEA 56X7 (Crockett)

2 SEA 56Y11 (Saavedra)

2 SEA 56Y13 (Wagner)

1 SEA 92R (DiGiovanni)

Copies

12 DTIC

2 University of Iowa

1 L. Landweber

1 A.T. Chwang

1 Virginia Polytechnic Inst.

1 D. Walker

CENTER DISTRIBUTION

Copies	Code	Name	Copies	Code	Name
1	0113	Douglas	1	2720	Hatchard
1	0114		1	2720	Skruch
1	0115		1	2720	Urbach
1	0117	Nakonechny	1	2721	Stricker
1	15	Morgan	1	2721	Purnell
1	1506	Walden	1	2722	Helmick
1	1508	Boswell	10	2722	Bein
1	154	McCarthy	1	274	Wang
1	1542	Huang	1	2741	Henry
20	1542	Lee	1	2741	Calvert
10	1542	Jiang	1	522.1	TIC (C)
1	1544	Peterson	1	522.2	TIC (A)
1	1544	Dai	1	5231	Office Services
1	1544	Kim			
1	156	Cieslowski			
1	1563	Milne			
1	1563	Moran			
1	1564	Feldman			
1	1905	Blake			
1	27	Argiro			
1	27B	Cox			
1	2704	Hwang			
1	2704	Quandt			
1	272	Ward			